Natural Gum-Assisted Phthalocyanine Immobilization in Electroactive Nanocomposites: Physicochemical Characterization and Sensing Applications

Maysa F. Zampa,[†] Ana Cristina F. de Brito,[‡] Igor L. Kitagawa,[§] Carlos J. L. Constantino,[§] Osvaldo N. Oliveira Jr.,[||] Helder N. da Cunha,[⊥] Valtencir Zucolotto,[||] José Ribeiro dos Santos Jr.,[†] and Carla Eiras*[,†]

DQ and DF, UFPI, CCN, 64049-550, Teresina, PI, Brazil, DQ, UFC, 60455-760, Fortaleza-CE, Brazil, DFQB, FCT, UNESP, CP 467, 19060-900, Presidente Prudente, SP, Brazil, IFSC, USP, CP 369, 13560-970, São Carlos, SP, Brazil

Received May 14, 2007; Revised Manuscript Received August 15, 2007

Natural gums have been traditionally applied in cosmetics and the food industry, mainly as emulsification agents. Due to their biodegradability and excellent mechanical properties, new technological applications have been proposed involving their use with conventional polymers forming blends and composites. In this study, we take advantage of the polyelectrolyte character exhibited by the natural gum Chichá (*Sterculia striata*), extracted in the Northeastern region of Brazil, to produce electroactive nanocomposites. The nanocomposites were fabricated in the form of ultrathin films by combining a metallic phthalocyanine (nickel tetrasulfonated phthalocyanine, NiTsPc) and the Chichá gum in a tetralayer architecture, in conjunction with conventional polyelectrolytes. The presence of the gum led to an efficient adsorption of the phthalocyanine and enhanced the electrochemical response of the films. Upon combining the electrochemical and UV−vis absorption data, energy diagrams of the Chichá/NiTsPc-based system were obtained. Furthermore, modified electrodes based on gum/phthalocyanine films were able to detect dopamine at concentrations as low as 10^{-5} M.

Introduction

The polysaccharide extracted from the Chichá tree (*Sterculia striata*)[1−3] is a natural gum whose main function is to protect the tree against infections and/or wounds. These gums are classified as hydrocolloids, with applications in cosmetics and the food industry, mainly as emulsification agents.[2,4] Chichá gum, in particular, is a heteropolymer containing partially acetylated chains and a high concentration of uronic acid (42.2%), galactosis (23.4%), rhamnose (28.8%), and xylose (5.6%).[1] This gum is found in several regions of Brazil, including the states of Piauí, Bahia, Minas Gerais, Goiás, and Amazonas. The polyanionic character of this gum arises from the presence of carboxylic acid groups, through which intermolecular interactions may occur.[1,2] The technological interest in the Chichá gum, which has been proven to be compatible with many synthetic polymers, comes mainly from its biodegrability and mechanical properties.

Metallic phthalocyanines are macrocyclic molecules bearing a central atom with high electronic density and reactivity.[5−7] Phthalocyanines may undergo chemical functionalization upon reaction via the central atom or the macrocycle with specific ligands, which make them candidate materials for sensors, catalysts, and optoelectronic and optical storage devices.[5,7,8] The incorporation of modified phthalocyanines in a polymeric matrix is an efficient strategy to obtain electroactive nanocomposites with distinct and optimized properties.[5,6] Recent studies have shown that sulfonated metallophthalocyanines may be assembled together with conventional polyelectrolytes or conducting polymers, using the layer-by-layer technique (LbL), for sensing and electronic applications.[9−12] The main advantage in processing phthalocyanines in the form of nanostructured layered composites is that film thickness and architecture may be controlled at the molecular level.[11]

In this study, LbL films were produced with nickel tetrasulfonated phthalocyanine (NiTsPc) and the natural gum Chichá. Since NiTsPc and Chichá are polyanions, the multilayer deposition was carried out in a tetralayer fashion in which a conventional cationic polyelectrolyte, viz., poly(allylamine hydrochloride) (PAH), was interposed between the polyanionic layers. The influence of the Chichá gum in the (PAH/Gum/PAH/NiTsPc)$_n$ nanocomposites (where n is the number of tetralayers) was investigated through electrochemical experiments. We also investigated the ability of the nanocomposites to act as modified electrodes for dopamine sensing.

Experimental Details

Materials. Chichá gum was extracted in Piauí State (Northeast region of Brazil) in August, 2004, and purified in the form of sodium salt as described elsewhere.[13] The detailed physicochemical characterization as well as the quantitative analysis of chemical composition of the gum employed here may be found in ref 1. After purification, 0.25 mL of ethanol was added to 5.0 g of gum, which was immediately dissolved in 100 mL of Milli-Q water under stirring for 24 h, followed by filtration. The final aqueous solution had a concentration of 50 mg/mL and pH 6.5 (pH was adjusted with 0.1 M HCl). All the reagents

* To whom correspondence should be addressed. E-mail: carla.eiras.ufpi@gmail.com.
[†] DQ, UFPI.
[‡] UFC.
[§] UNESP.
[||] USP.
[⊥] DF, UFPI.

10.1021/bm700528u CCC: $37.00
Published on Web 10/16/2007

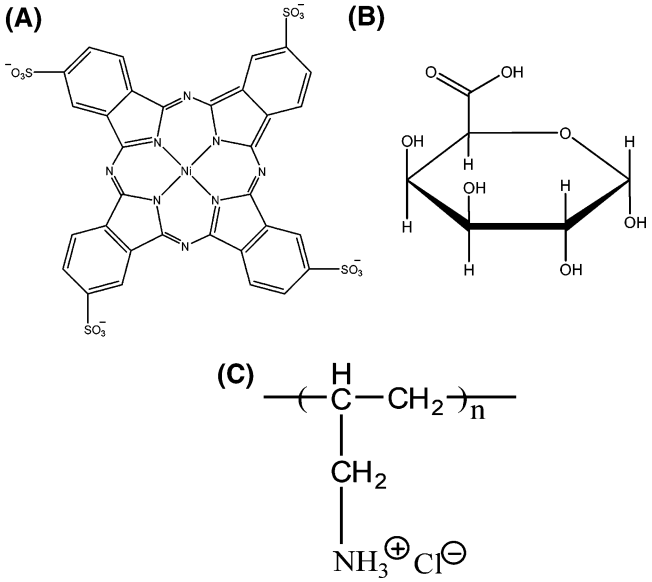

Figure 1. Chemical structures of (A) NiTsPc, (B) galacturonic acid (a major constituent of Chichá gum), and (C) poly(allilamine hydrochloride) (PAH).

were purchased from VETEC (Brazil), analytical grade. NiTsPc and PAH were purchased from Aldrich Co. and used without further purification in aqueous solutions at a concentration of 0.5 mg/mL and pH 2.5. The chemical structures of the materials employed are depicted in Figure 1.

Multilayer Deposition. Natural gum-containing films were adsorbed onto glass and glass covered with indium tin oxide (ITO) substrates in a tetralayer fashion. Two distinct architectures were investigated: $(PAH/Chichá/PAH/NiTsPc)_n$ (sequence 1) and $(PAH/NiTsPc/PAH/Chichá)_n$ (sequence 2), where n is the number of tetralayers. Multilayer films with $n = 2$, 5, 7, and 10 were obtained by immersing the substrate into the polycationic (PAH) or anionic (NiTsPc or Chichá) solutions (according to the architecture desired) during 5 min. After deposition the substrates were rinsed in a washing solution and dried under a nitrogen flow. The growth of the multilayers was monitored with UV−vis spectroscopy by collecting the absorbance spectrum after each deposition step, using a Hitachi U-3000 spectrophotometer. The surface morphology of the LbL films at micrometer scale was characterized through micro-Raman spectroscopy using a Renishaw model in-Via equipped with a 785 nm laser line, CCD detector 1200 L/mm grating, XYZ motorized stage, and a Leica optical microscope with lens of 5×, 20×, and 50×, which allow collecting the spectra from areas of 1 μm^2.

Cyclic Voltammetry. Cyclic voltammograms were collected with LbL films deposited onto ITO using a potentiostat Autolab PGSTAT 30 Eco Chemie and a 10.0 mL, three-electrode electrochemical cell. The reference electrode was an Hg/HgCl/KCl(sat.) (SCE); a 1.0 cm^2 platinum foil was used as auxiliary electrode. The LbL films deposited in the sequences 1 and 2 on ITO with an area of 0.4 cm^2 were employed as working electrodes. Experiments were carried out using a solution of 0.05 M H_2SO_4 or 0.1 M HCl at 22 °C. For comparison, cyclic voltammograms were obtained using LbL films with the architectures $(PAH/NiTsPc)_m$, $(NiTsPc/PAH)_m$, and $(PAH/Chichá)_m$ as working electrodes, where m is the number of bilayers. Cyclic voltammetry was also employed for detecting dopamine (DA), with DA being added in the electrolytic solution in a concentration range from 0.25 to 30 × 10^{-5} M.

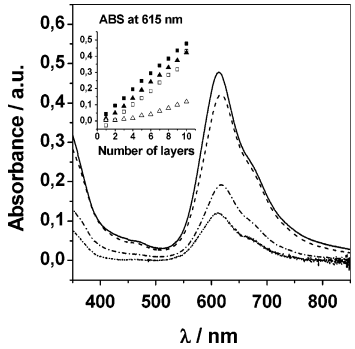

Figure 2. UV−vis absorption spectra for 10-bi-/-tetralayer films of (−; ■) PAH/Chichá/PAH/NiTsPc (sequence 1); (--; □) PAH/NiTsPc/PAH/Chichá (sequence 2); (− · −; ▲) PAH/NiTsPc and (···; △) NiTsPc/PAH. Inset: Linear increment of the absorption at 615 nm as a function of the number of bi-/tetralayers.

Results and Discussion

Film Growth and Spectroscopic Characterization. The electronic absorption spectra for 10-bilayer and 10-tetralayer LbL films assembled according to the different architectures are shown in Figure 2. For tetrasulfonated phthalocyanines, the Q-band absorption is affected by aggregation of the substituent groups, which may lead to shift and broadening of the absorption band.[5] Absorption in the visible region at ca. 615 nm is only due to the NiTsPc layer, since PAH and Chichá do not absorb in this region. No significant differences are observed in the electronic absorption of 10-tetralayer films comprising architectures 1 or 2, where the band at 615 nm is evidence of dimeric species, whereas the shoulder at 654 nm is indicative of monomeric species.[5] Note also that films containing 10 bilayers of PAH/NiTsPc (without gum) exhibited lower absorption, suggesting that Chichá enhances adsorption of NiTsPc. The linear increment in the absorbance as a function of the number of deposited tetralayers or bilayers is shown in the inset of Figure 2, suggesting that the same amount of material was adsorbed in each deposition step. The higher deposition efficiency of the tetralayer architecture is due to the interposition of Chichá gum in the multilayers, which increase the amount of adsorbed PAH molecules (if compared with films containing only PAH/NiTsPc), resulting in a higher number of NH_3^+ sites available for NiTsPc binding.[10] The architecture used to assemble the tetralayer films also affects the amount of material adsorbed, which is higher in sequence 1 (PAH/Chichá/PAH/NiTsPc). Complementary, Figure 3 shows the optical images for both LbL films (sequences 1 and 2) collected with a lens of 50× magnification and their Raman spectra recorded using the 785 nm laser line. The spectra of Chichá and NiTsPc forming cast films are presented as reference of pure materials (the PAH did not present a significant Raman scattering). It can be seen that the morphology of the LbL films is homogeneous at the surface within the micrometer scale. This homogeneity is observed not only in terms of the morphology but also in terms of the spatial distribution of the materials that form the LbL films as revealed by the similarity among the several Raman spectra recorded along the LbL films.

Electrochemical Characterization. The electroactivity of LbL films containing Chichá and NiTsPc assembled in sequences 1 and 2 were studied using cyclic voltammetry, and the results are depicted in Figure 4. For comparison, a film containing only PAH/NiTsPc was also investigated. Although Chichá is not electroactive, its presence in the film leads to a higher electrochemical response (ca. 3× higher), in comparison to PAH/NiTsPc films, probably due to the higher amount of

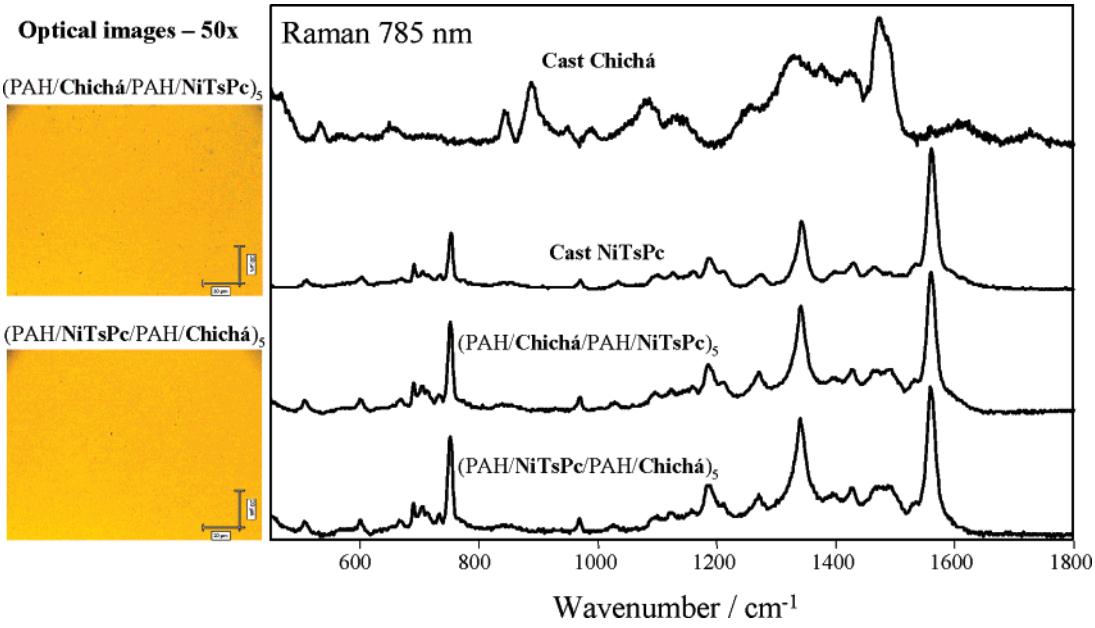

Figure 3. Optical images collected using a 50× magnification objective lens and Raman spectra recorded using the 785 nm laser line for the tetralayered LbL films (sequences 1 and 2). The Raman spectra for the pure Chichá and NitsPc forming cast films are presented as well.

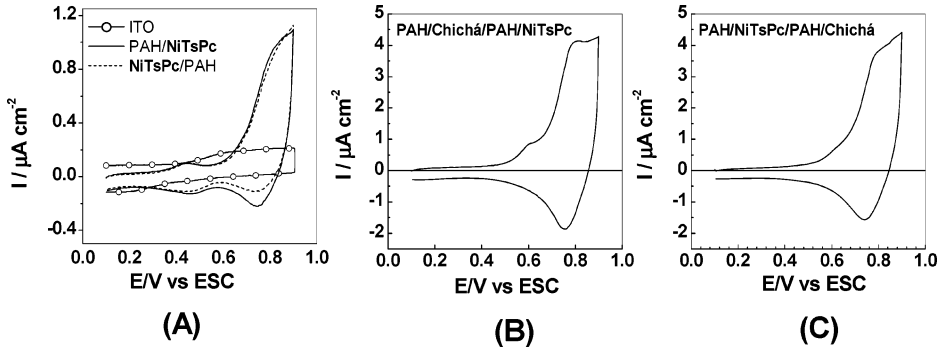

Figure 4. Cyclic voltammograms for (A) Bare ITO, ITO/$(PAH/NiTsPc)_{5bilayers}$, and ITO/$(NiTsPc/PAH)_{5bilayers}$; (B) ITO/$(PAH/Chichá/PAH/NiTsPc)_{5tetralayers}$; and (C) ITO/$(PAH/NiTsPc/PAH/Chichá)_{5tetralayers}$. Electrolytic solution: 0.05 M H_2SO_4; 50 mV s^{-1}.

Table 1. Oxidation Potentials for Bi- or Tetralayered Films

films	E_{p1} (V)	E_{p2} (V)
$ITO/(PAH/NiTsPc)_5$	0.45	0.85
$ITO/(PAH/Chichá/PAH/NiTsPc)_5$	0.61	0.80
$ITO/(PAH/NiTsPc/PAH/Chichá)_5$	not observed	0.80

NiTsPc present in the tetralayer architecture. Tetralayers assembled in sequence 1 exhibited two oxidation processes, where the first one at ca. 0.61 V comes from the metal center [Ni(II)/Ni(III) + e^-].[5] In this case, reduction must occur via electrons injected from the film layers, rather than the electrolytic solution, since a corresponding reduction peak was not observed in the voltammograms. Note that oxidation of the metal center (at ca. 0.61 V) was not observed in films assembled in sequence 2, probably because of a hindering effect caused by the Chichá outermost layer. The second process at 0.8 V is due to the oxidation of the Pc ring, with a corresponding reduction peak at ca. 0.75 V.[5,7] Significantly, the redox processes are better defined in films with sequence 1, which contain NiTsPc molecules atop.

The oxidation potentials are shown in Table 1. The redox processes are better defined in films fabricated with sequence 1. Tetralayered films (assembled in sequence 1 or 2) exhibited a catalytic effect, since the macrocycle oxidation peak shifted to lower potentials (0.8 V) in comparison to the bilayer films, for which this process occurred at 0.85 V. Surprisingly, an opposite effect was observed for the oxidation potential of the metal center (E_{p1}). Tetralayered films with sequence 1 exhibited E_{p1} = 0.61 V, whereas in the bilayer PAH/NiTsPc film (containing no gum) E_{p1} was 0.45 V. The latter may be indicative that the electron-acceptor groups (such as carboxylic groups) in the gum react with the phthalocyanine, reducing the charge of the Pc macrocycle, in a way that a higher potential is required for the oxidation of the metal center.[14] The electrochemical stability of the films was investigated in five-tetralayer films (sequence 1) subjected to 20 voltammetric cycles. As shown in Figure 5, peak currents decreased slightly, being practically constant after five cycles.

The reversibility of the Pc/gum-modified electrodes may be inferred from the following findings: (i) the anodic peak current (I_{pa}) varied linearly with the scan rate (Figure 6), (ii) there is no change in the anodic and cathodic potentials with the scan rate, and (iii) the difference between anodic and cathodic potentials is lower than 59 mV.[15,16] The linear dependence of the anodic current on the scan rate, shown in the inset of Figure 6, is evidence that the reaction is charge-transfer-controlled.[15] In this case, charge transfer occurs via electron hopping between neighboring redox sites within the multilayers from the redox center to the ITO electrode surface, under an applied potential.[17] Since the PAH/Chichá/PAH/NiTsPc (sequence 1) film exhibited the best electrochemical response, it was employed in further electrochemical studies, including detection of DA.

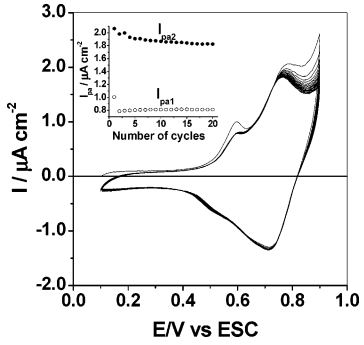

Figure 5. Electrochemical response for a ITO/(PAH/Chichá/PAH/NiTsPc)$_5$ electrode subjected to 20 voltammetric cycles in 0.05 M H_2SO_4, 50 mV s^{-1}. Inset: Dependence on the anodic peak current and number of cycles.

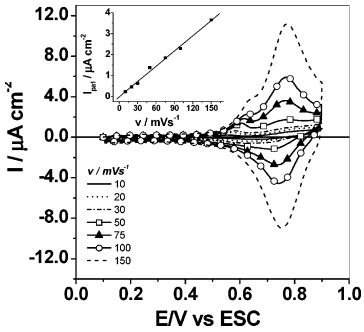

Figure 6. Cyclic voltammograms at several scan rates for a ITO/(PAH/Chichá/PAH/NiTsPc)$_5$. Inset: I_{pa_1} as a function of scan rate.

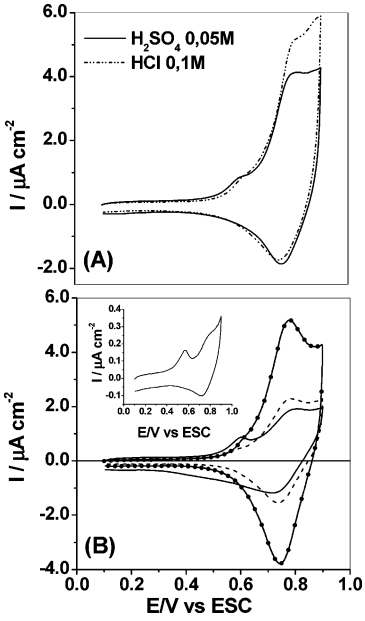

Figure 7. Cyclic voltammograms for (A) ITO/(PAH/Chichá/PAH/NiTsPc)$_5$ film collected in 0.05 M H_2SO_4 and 0.1 M HCl (as indicated) and (B) ITO/(PAH/Chichá/PAH/NiTsPc) films containing (−) 5, (--) 7, and (- • -) 10 tetralayers. Electrolytic solution: 0.05 M H_2SO_4. Scan rate: 50 mV s^{-1}. The inset shows the electrochemical response for the same system containing two tetralayers.

The influence of the electrolytic solution[18] on the electrochemical response of the films was investigated for a five-tetralayer PAH/Chichá/PAH/NiTsPc using 0.05 M H_2SO_4 or 0.1 M HCl as the electrolytic solution, as shown in Figure 7A. The redox processes at 0.61 and 0.8 V (from metal center and macrocycle, respectively) are better defined using 0.05 M H_2SO_4. Because charge in the ion HSO_4^- is located at the peripheral region, the electrostatic attraction of water molecules is increased, thus causing the ions to be more hydrated, exhibiting a lower conductance and mobility in comparison to the Cl^- ions. As a consequence, the electroactive sites of the film are preserved upon potential application, and a better peak definition may be achieved. In all the subsequent experiments, 0.05 M H_2SO_4 was employed as electrolytic solution.

Table 2. Parameters Employed for Energy Diagram Fabrication of the ITO/(PAH/Chichá/PAH/NiTsPc) System

parameter	value	parameter	value
E'_{ox} (V vs ESC)	0.5	E_g (eV)	1.7
PI (eV)	5.2	EA (eV)	3.5
λ' (nm)	732		

It has been reported[9,10] that the electroactivity of LbL films depends strongly on the amount of electroactive material and permeability of the electrolyte within the multilayers. The dependence of the electrochemical response on the number of tetralayers is shown in Figure 7B for a film assembled according to sequence 1. As expected, the peak current increased with the number of tetralayers due to the higher number of electroactive sites available. However, the oxidation peak from the metallic center is less defined for films containing 7 and 10 tetralayers. A good balance between current intensity and peak definition may be achieved in the five-tetralayer PAH/Chichá/PAH/NiTsPc film.

The reversibility and stability of the gum-based films, especially the PAH/Chichá/PAH/NiTsPc electrode, made it possible to produce an energy diagram[17,19,20] by obtaining the ionization potential (IP), electroaffinity (EA), and gap energy (E_g).[19−21] IP and EA determine the interfacial energy barrier between the electrode and the electroactive molecule and are usually used to optimize the performance of electronic devices.[16,19,20] They may be estimated from the electrochemical potentials measured after correcting the potential obtained with SCE electrodes using the vacuum level referenced to 4.7 [16] eV. First, the oxidation potential (E_{ox}) relative to the vacuum level was calculated using eq 1, with the onset potential estimated from the intersection of the two slopes drawn at the rising oxidation current and background current in the cyclic voltammograms (E'_{ox}) (not shown).[19,20]

$$E_{ox} = E'_{ox} + E_{ESC} \approx E'_{ox} + E_{vac} + 4.7 \qquad (1)$$

Assuming $E_{vac} = 0$, then IP $= eE_{ox}$, where e is the elementary charge, it is possible to estimate the HOMO (highest occupied molecular orbital) in the energy diagram.[19−21] The energy of electronic transitions (E_g) of the PAH/Chichá/PAH/NiTsPc film was estimated according to

$$E_g = \frac{hc}{\lambda'} \qquad (2)$$

where h is the Planck constant, c is the light speed, and λ' is the initial wavelength. λ' may be obtained from the intersection of the two slopes drawn at the maximum absorption and background absorption in the electronic spectra. Finally, EA may be obtained upon subtracting E_g from IP (EA = IP − E_g). Table 2 summarizes the parameters obtained. The high value obtained for the HOMO energy, shown in the schematic diagram of Figure 8, suggests that a positive potential must be applied in the oxidation of polymeric electrodes containing NiTsPc, PAH, and Chichá. The latter agrees with reports on the fabrication of modified electrodes using metallic phthalocyanines.[16,19]

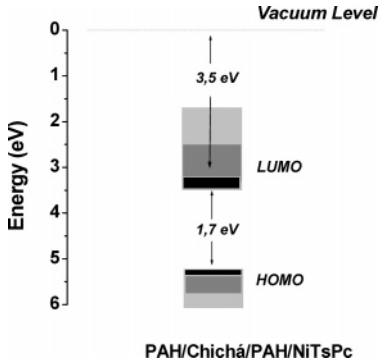

Figure 8. Proposed energy diagram for ITO/(PAH/Chichá/PAH/NiTsPc)$_5$ LbL film.

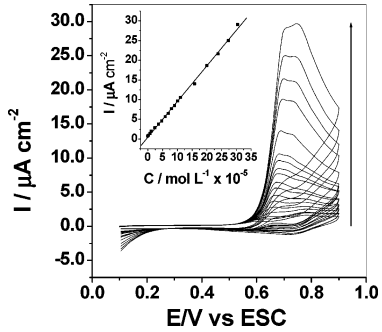

Figure 9. Electrochemical response of an ITO/(PAH/Chichá/PAH/NiTsPc)$_5$ electrode in the presence of different amounts of DA in the electrolytic solution (0.05 M H_2SO_4) at 50 mV s^{-1}. Inset: Linear dependence of I_{pa1} as a function of DA concentration.

The use of LbL films as modified electrodes for electrochemical sensing has been reported in the literature. The main advantages in using these films are the low detection limits and absence of residues.[22,23] A five-tetralayer PAH/Chichá/PAH/NiTsPc (sequence 1) film was employed here as a modified electrode for DA detection. The DA oxidation through a two-electron process[24,25] was evidenced by the increase in the peak current upon addition of DA in the electrochemical cell during the voltammetric measurements, as shown in Figure 9. DA was added with concentrations ranging from 0.25 to 30 $\times$ 10^{-5} M. The calibration curve was obtained using linear regression, with a correlation coefficient of 0.999, according to

$$I_{pa}\,(\mu A) = 0.476 + 0.905 \times 10^5\,C \qquad (3)$$

The detection limit[26] (DL) was estimated as 1.05 $\times$ 10^{-5} M, which is in good agreement with previously reported results.[9,25,27] For example, detection limits of 10^{-5} M have been reported by Siqueira et al., for LbL films of chitosan assembled with three types of sulfonated phthalocyanines containing iron (FeTsPc), nickel (NiTsPc), or copper (CuTsPc).[27] In the latter, it was also observed that only the chitosan/CuTsPc and chitosan/FeTsPc films were able to distinguish between DA and ascorbic acid (AA), which is a natural interferent for DA.

The DA oxidation mechanism was investigated by varying the scan rate between 10 and 150 mV s^{-1}, using the higher DA concentration of 30 $\times$ 10^{-5} M. The quadratic dependence of the peak current on the scan rate in Figure 10 points to a diffusional mechanism.[15] The process is completely reversible, i.e., the peak current returned to the initial values if the film was cycled again in a DA-free electrolytic solution, after film washing. The latter is illustrated in Figure 11, where voltammograms for a bare-ITO electrode are also shown. For comparison, DA detection was also carried out using a five-bilayer PAH/NiTsPc film under the same experimental conditions described above (not shown), and the results are summarized in Table 3. It can be seen that as far as the DA detection is concerned, electrodes bearing a bilayer architecture are advantageous due to the lower limit of detection exhibited by these systems.

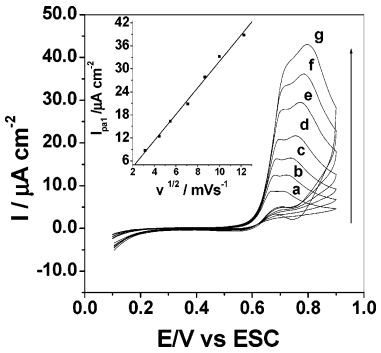

Figure 10. Electrochemical response of a five-tetralayer PAH/Chichá/PAH/NiTsPc (sequence 1) in the presence of 30 $\times$ 10^{-5} M DA at different scan rates: (a) 10, (b) 20, (c) 30, (d) 50, (e) 75, (f) 100, and (g) 150 mV s^{-1}. Inset: Linear dependence of the I_{pa1} as a function of $v^{1/2}$.

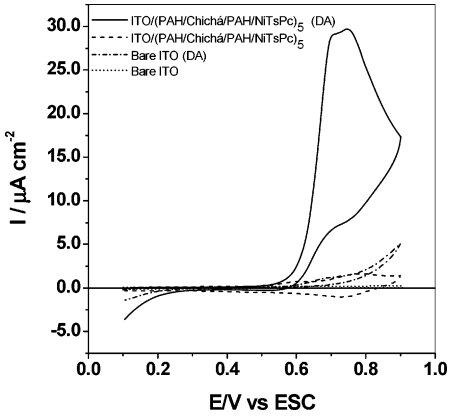

Figure 11. Cyclic voltammograms comparing the electrochemical response of a bare ITO, ITO/(PAH/Chichá/PAH/NiTsPc)$_5$, and ITO/(PAH/NiTsPc)$_5$ modified electrodes in the absence and in the presence of 30 $\times$ 10^{-5} M DA, as indicated.

Table 3. Detection Limit (DL), I_{pa_1}, and Oxidation Potential for Different Electrodes Subjected to DA Detection[a]

electrodes	DL (M)	$I_{pa}1$ (μA)	E (V)
(PAH/NiTsPc)$_5$	8.9 $\times$ 10^{-7}	28.79	0.70
(PAH/Chichá/PAH/NiTsPc)$_5$	1.05 $\times$ 10^{-5}	29.43	0.68

[a] All of the electrodes presented reversibility after washing.

Conclusions

Supramolecular structures containing natural polyelectrolyte gums and metallophthalocyanines were assembled using the LbL technique in two tetralayer architectures. Both tetralayered LbL films are homogeneous at the micrometer scale, either morphologically or chemically. However, the LbL film assembled in sequence 1 exhibited the best electrochemical response and the films displayed good electrochemical stability and reversibility. The latter allowed the estimation of the system HOMO energy. On the basis of cyclic voltammetry and reports from the literature, we could infer that charge transfer within the multilayered architecture probably occurs via electron hopping.

The tetralayer films containing Chichá did not show advantages in terms of dopamine detection, in comparison with PAH/NiTsPc bilayered films that reached lower detection limits (on the order of 10^{-7} M). On the other hand, the presence of the natural gum was advantageous for both film assembly and electroactivity, since redox currents were higher for films containing the Chichá gum (in comparison to PAH/NiTsPc films).

The possibility of assembling natural gums with semiconductor organic molecules opens up new prospects for using these natural biodegradable materials in technological applications.

Acknowledgment. The authors thank FAPEPI, FAPESP, CAPES, CNPq, and IMMP/MCT for financial support. Technical support from LAPETRO is also acknowledged. We are also grateful to Dr. Wânia Moreira (UFSCar, Brazil) for its helpful discussions.

References and Notes

(1) Brito, A. C. F.; Silva, D. A.; Paula, R. C. M.; Feitosa, J. P. A. *Sterculia striata* exudate polysaccharide: characterization, rheological properties and comparison with *Sterculia urens* (karaya) polysaccharide. *Polym. Int*. **2004,** *53*, 1025−1032.

(2) Brito, A. C. F.; Sierakowski, M. R.; Reicher, F.; Feitosa, J. P. A.; Paula, R. C. M. Dynamic rheological study of *Sterculia striata* and karaya polysaccharides in aqueous solution. *Food Hydrocolloids* **2005,** *19*, 861−867.

(3) Silva, D. A.; Brito, A. C. F.; Paula, R. C. M.; Feitosa, J. P. A.; Paula, H. C. B. Effect of mono and divalent salts on gelation of native, Na and deacetylated *Sterculia striata* and *Sterculia urens* polysaccharide gels. *Carbohydr. Polym.* **2003**, *54*, 229−236.

(4) Verbeken, D.; Dierckx, S.; Dewettinck, K. Exudate gums: occurrence, production, and applications. *Appl. Microbiol. Biotechnol*. **2003,** *63*, 10−21.

(5) Leznoff, C. C.; Lever, A. B. P.; *Phthalocyanines*—Properties and applications, Vols. 1−3; John Wiley & Sons: New York, 1989.

(6) Toma, H. E. *O mundo nanométrico: A dimensão do novo século*; Oficina de Textos: S˜ao Paulo, Brazil, 2004.

(7) Irvine, J. T. S.; Eggins, B. R. The cyclic voltammetry of some sulphonated transition metal phthalocyanines in dimethylsulphoxide and in water. *J. Electroanal. Chem*. **1989,** *271*, 161−172.

(8) Nevin, W. A.; Liu, W.; Melnik, M.; Lever, A. B. P. Spectroelectrochemistry of cobalt and iron tetrasulphonated phthalocyanines. *J. Electroanal. Chem*. **1986,** *213*, 217−234.

(9) Zucolotto, V.; Ferreira, M.; Cordeiro, M. R.; Constantino, C. J. L.; Moreira, W. C.; Oliveira, O. N., Jr. Nanoscale manipulation of polyaniline and phthalocyanines for sensing applications. *Sens. Actuators, B* **2006**, *113*, 809−815.

(10) Paterno, L. G.; Mattoso, L. H. C.; Oliveira, O. N., Jr. Filmes poliméricos ultrafinos produzidos pela técnica de automontagem: Preparação, propriedades e aplicações. *Quim. Nova* **2001**, *24*, 228−235.

(11) Zucolotto, V.; Ferreira, M.; Cordeiro, M. R.; Constantino, C. J. L.; Balogh, D. T.; Zanatta, A. R.; Moreira, W. C.; Oliveira, O. N., Jr. Unusual interactions binding iron tetrasulfonated phthalocyanine and poly(allylamine hydrochloride) in layer-by-layer films. *J. Phys. Chem. B* **2003**, *107*, 3733−3737.

(12) Schönhoff, M. Self-assembled polyelectrolyte multilayers. *Curr. Opin. Colloid Interface Sci*. **2003**, *8*, 86−95.

(13) Costa, S. M. O.; Rodrigues, J. P. A.; De Paula, R. C. M. Monitorização do processo de purificaç˜ao de gomas naturais: goma do cajueiro. *Rev. Bras. Eng. Agríc. Ambient.* **1996**, *2*, 49−54.

(14) (14) Santos, J. R., Jr. Propriedades eletroquímicas de ftalocianinas de ferro e cobalto para a redução de oxigênio. Master's Dissertation, University of São Paulo, Brazil, 1991.

(15) Brett, C. M. A.; Brett, A. M. O. Electroquímica: princípios, métodos e aplicações, Vol. 1; Almedina: Coimbra, Portugal, 1996.

(16) Bard, A. J.; Faulkner, L. R. *Electrochemical methods: Fundamentals and applications*, 2nd ed.; John Wiley & Sons: New York.

(17) Crespilho, F. N.; Zucolotto, V.; Oliveira, O. N., Jr.; Nart, F. C. Electrochemistry of layer-by-layer films: A review. *Int. J. Electrochem. Sci*. **2006**, *1*, 194−214.

(18) Agostinho, S. M. L.; Villamil, R. F. V.; Agostinho Neto, A.; Aranha, E. O eletrólito de suporte e suas múltiplas funções em processos de eletrodo. *Quim. Nova* **2004**, *27*, 813−817.

(19) Crespilho, F. N.; Zucolotto, V.; Siqueira, J. R., Jr.; Carvalho, A. J. F.; Nart, F. C.; Oliveira, O. N., Jr. Using electrochemical data to obtain energy diagrams for layer-by-layer films from metallic phthalocyanines. *Int. J. Electrochem. Sci*. **2006**, *1*, 151−159.

(20) Micaroni, L.; Nart, F. C.; Hummelgen, I. A. Considerations about the electrochemical estimation of the ionization potential of conducting polymers. *J. Solid State Electrochem.* **2002**, *7*, 55−59.

(21) Chen, Y.; O'Flaherty, S. M.; Hanack, M.; Blau, W. J. New axially aryloxy substituted gallium phthalocyanines for nonlinear optics. *J. Mater. Chem*. **2003**, *13*, 2405−2408.

(22) Lawrence, N. S.; Beckett, E. L.; Davis, J.; Compton, R. G. Advances in the voltammetric analysis of small biologically relevant compounds. *Anal. Biochem*. **2002**, *303*, 1−16.

(23) Skoog, D. A.; Holler, F. J. *Princípios de análise instrumental*, 5th ed.; Bookman: 2002.

(24) Oni, J.; Nyokong, T. Simultaneous voltammetric determination of dopamine and serotonin on carbon paste electrodes modified with iron(II) phthalocyanine complexes. *Anal. Chim. Acta* **2001**, *434*, 9−21.

(25) Ferreira, M.; Dinelli, L. R.; Wohnrath, K.; Batista, A. A. A.; Oliveira, O. N., Jr. Langmuir−Blodgett films from polyaniline/ruthenium complexes as modified electrodes for detection of dopamine. *Thin Solid Films* **2004**, *446*, 301−306.

(26) Lanças, F. M. Validação de métodos cromatográficos de análise; Rima: São Carlos, Brazil, 2004.

(27) Siqueira, J. R., Jr.; Gasparotto, L. H. S.; Crespilho, F. N.; Carvalho, A. J. F.; Zucolotto, V.; Oliveira, O. N., Jr. Physicochemical properties and sensing ability of metalophtalocyanines/chitosan nanocomposites. *J. Phys. Chem. B* **2006**, *110*, 22690−22694.

BM700528U